Biophysical Chemistry, 48 (1993) 171–182
Elsevier Science Publishers B.V., Amsterdam

BIOCHE 01799

Molten globule monomers in human superoxide dismutase

Norberto Silva, Jr. [a,*], Enrico Gratton [b], Giampiero Mei [c], Nicola Rosato [c], Ruth Rusch [d] and Alessandro Finazzi-Agrò [c]

[a] *Mayo Clinic, Guggenheim 14, 200 First St., SW, Rochester, MN 55905 (USA)*
[b] *Laboratory for Fluorescence Dynamics, Department of Physics, University of Illinois at Urbana-Champaign, 1110 West Green Street, Urbana, IL 61801 (USA)*
[c] *Dipartimento di Medicina Sperimentale e Scienze Biochimiche, Università di Roma "Tor Vergata", Via O. Raimondo 8, 00173 Rome (Italy)*
[d] *Brown University, Biomedical Department, P.O. Box G, Providence, RI 02912 (USA)*

(Received 23 April 1993; accepted 13 July 1993)

Abstract

The time-resolved fluorescence decay and anisotropy of Cu/Zn human superoxide dismutase (HSOD) were studied as a function of temperature and denaturant concentration. In addition, circular dichroism (CD) measurements were performed on HSOD as a function of denaturant concentration in the amide and aromatic regions. The time-resolved fluorescence decay results reveal the existence of structural microheterogeneity in HSOD. Furthermore, CD measurements and a global analysis decomposition of the time-resolved fluorescence decay over denaturant concentration shows the presence of an intermediate in the unfolding of HSOD by guanidinium hydrochloride. Considering our previous measurements of partially denatured HSOD as a function of protein concentration (Mei et al., Biochemistry 31 (1992) 7224–7230), our results strongly suggest that the unfolding intermediate is a monomer that displays a molten globule state.

Keywords: Human superoxide dismutase; Time-resolved fluorescence; Global analysis; Conformational substates; Molten globule state

1. Introduction

Protein folding is biologically important for many reasons. For instance, folding is necessary to initiate the function of various precursor enzymes [1]. Furthermore, protein folding intermediates may be necessary for protein translocation across cell membranes [3]. Finally, knowledge of protein folding could provide avenues toward designing novel enzymes [1].

Current research has established that some proteins exhibit an intermediate state during the folding/unfolding process [4–7]. Experimental methods confirming the existence of intermediates include circular dichroism (CD), nuclear magnetic resonance, infrared spectroscopy and intrinsic viscosity measurements [8–11]. In addition, another powerful method for investigating protein folding intermediates is through the fluo-

* Corresponding author. Fax (507) 284-9349.

[1] Abbreviations: Circular dichroism (CD), human superoxide dismutase (HSOD), guanidine hydrochloride (GdHCl), tryptophan (Trp).

rescence decay of extrinsic and intrinsic probes [6, 11, 12].

Steady-state and time-resolved fluorescence studies have illuminated many differences between native and denatured proteins [12, 13–15]. One general result from time-resolved fluorescence studies of denatured proteins is the increased heterogeneity in conformation as compared to the native state [15–17]. This result has been confirmed by our studies on the single tryptophan fluorescence decay of human superoxide dismutase (HSOD). HSOD is an ideal system to study protein denaturation because: (1) it contains a single Trp residue per monomer unit (HSOD is a dimer with identical subunits [18]), which simplifies interpretive analysis, and (2) Trp is environmentally sensitive making it an ideal reporter of microheterogeneity. Our results have shown that the time-resolved fluorescence decay of denatured HSOD in 6.5 *M* guanidine hydrochloride (GdHCl) displays more heterogeneity than that of native HSOD [1]. These studies also showed that the native form of HSOD displays structural microheterogeneity. This is in agreement with the concept of protein conformational substates in systems such as myoglobin [19–21]. Finally, our HSOD studies suggest that the monomerization stage of HSOD displays a molten globule state. The molten globule state is a protein folding intermediate of considerable interest which is characterized as having native-like secondary structure and fluctuating tertiary structure [11, 22]. There is also theoretical evidence for the existence of a molten globule state in proteins [23].

However, our previous evidence for a HSOD molten globule state were limited to experiments at a single temperature (20°C). Furthermore, a full decomposition of the time-resolved fluorescence decay was not done with an intermediate in mind. This decomposition is crucial if we are to suspect that the intermediate displays properties which are characteristic of a molten globule state. In addition, previous time-resolved fluorescence measurements were only correlated to the amide CD signal of HSOD. In this article we have extended the CD measurements to the aromatic region which is a key test for the existence of a molten globule state in HSOD. In addition, a two-dimensional experiment has been performed to rigorously test the hypothesis of structural microheterogeneity and the existence of a molten globule state. This involves time-resolved fluorescence decay experiments of HSOD over denaturant concentration *and* temperature. The temperature and denaturant range covered is relatively broad (10°C to 50°C and 0.0 *M* to 6.5 *M* GdHCl) and the interval between experiments is relatively small (5°C and 0.5–1.0 *M* GdHCl). For this work we plan to perform a global analysis of the time-resolved fluorescence decay of HSOD over denaturant concentration to test the existence of an intermediate. Time-resolved fluorescence anisotropy decay measurements were also performed as a function of temperature and denaturant concentration. The time-resolved fluorescence anisotropy measurements monitor the "fluidity" of the environment of the Trp residue in HSOD as a function of GdHCl concentration.

2. Experimental

2.1. Sample preparation

Holo-HSOD was purified from human erythrocytes [24]. Samples were dissolved in 0.01 *M* potassium phosphate buffer at pH 7.6. Denaturation was accomplished by mixing an appropriate amount of HSOD stock solution with ultra-pure guanidine hydrochloride (from ICN Biomedical, Inc., Cleveland, OH, USA). The final protein concentration was around 30 μM giving an approximate optical density of 0.1 at 295 nm. The following concentrations of GdHCl were used: 0.0, 1.0, 2.0, 3.0, 3.5, 4.0, 4.5, 5.0, 5.5, 6.0 and 6.5 *M* (time-resolved fluorescence anisotropy measurements were not done at 5.5 *M* GdHCl). At each denaturant concentration temperature dependent experiments were performed from 10°C to 50°C in steps of 5°C. The temperature was monitored continuously during measurements by attaching a thermocouple to the sample cuvette. The readings of the thermocouple were monitored by an Omega Digicator (from Omega Engineering, Stamford, CT, USA) with an accuracy of ±0.1°C.

2.2. Time-resolved fluorescence and anisotropy measurements

All time-resolved fluorescence and anisotropy measurements were performed at the Laboratory for Fluorescence Dynamics of the University of Illinois at Urbana-Champaign, Urbana, IL, USA. Frequency domain techniques were used to measure the fluorescence decay of all samples in the range of 10 to 240 MHz [25]. The light source was a high repetition mode-locked Nd-YAG laser used to pump a rhodamine dye laser yielding a 10 ps pulse output of about 50 mW at 590 nm with a 2 MHz repetition rate. This output was then frequency doubled to 295 nm and its harmonic content was used to excited the sample [26]. The excitation was polarized at the "magic angle" to eliminate rotational effects on the fluorescence lifetime measurements [27]. The emission was observed using an optical filter combination of UV34 and U340 (from Oriel Corp., Stratford, CT, USA).

2.3. Circular dichroism measurements

Circular dichroism measurements were carried out using a Jobin- Yvon CD VI spectropolarimeter (from SPEX Industries, Inc., Edison, NJ, USA). The sample holder was thermostated at 20°C using an external bath circulator. Measurements of the amide CD of HSOD were performed as a function of GdHCl concentrations in our previous study [1]. These samples were in the concentration range 0.1–1.0 mg/ml and the samples were placed in 1.0 cm quartz cuvettes. Aromatic CD measurements of HSOD were performed as a function of GdHCl concentration in this study. Samples for measuring the aromatic CD were in the concentration range of 2–3 mg/ml since this signal is weak at lower concentrations.

2.4. Analysis and graphical presentation of data

Data analysis was performed by minimizing the reduced χ^2 with a routine based on the Marquardt algorithm using the Globals Unlimited software [28]. The results of some of these fits are shown in three-dimensional graphs with the x- and y-axes corresponding to temperature and denaturant concentration, respectively. The temperature axis of these graphs correctly portrays the intervals between experiments (5°C). However, the GdHCl axis division does not completely reflect the experiments conducted on HSOD. In particular, no data was taken for 0.5, 1.5 and 2.5 M GdHCl for Figs. 2, 3, 4–6 and 11–13. In addition, no data was taken for 5.5 M GdHCl in Figs. 4–6. In addition, some of the data, being high in laser noise or having large systematic error, were discarded. A total of 10 experiments were removed from the time-resolved fluorescence decay data set (Figs. 2, 3 and 11–13) and a total of 12 experiments were removed from the time-resolved fluorescence anisotropy decay data set (Figs. 4–6). As a result, an interpolation was performed to fill in the missing data points in all three dimensional graphs. The corresponding interpolation points, (x,y), for the rejected data sets are listed as follow for Figs. 2, 3 and 11–13 where x is the temperature (in degrees Celsius) and y is the denaturant concentration (in m/l): (15,4.5), (20,4.5), (20,5.0), (25,5.0), (30,5.0), (45,5.0), (15,5.5), (20,5.5), (25,5.5) and (25,6.0). For Figs. 4–6 the rejected data sets are: (45,3.5), (15,4.5), (20,4.5), (20,5.0), (25,5.0), (30,5.0), (45,5.0), (50,5.0) (25,6.0), (35,6.0), (40,6.0), (50,6.0). Considering that the remaining number of time-resolved fluorescence decay experiments is 89 and the remaining number of time-resolved fluorescence anisotropy experiments is 78, this still leaves a high density of experimental points on the three dimensional graphs.

Correlated error analysis were also performed using the Globals Unlimited rigorous error analysis routine. The errors on the fluorescence decay parameters characterized by the center and width of the lifetime distribution are ± 0.03 ns and ± 0.05 ns, respectively (Figs. 2 and 3). The errors on the fluorescence anisotropy decay parameters (Figs. 4–6) characterized by the rotational diffusion coefficient of the protein, D_{pro}, the wobbling diffusion coefficient of the Trp residue, D_{Trp}, and the semi-cone angle, θ, are on the order of ± 0.005/ns, ± 0.02/ns, and $\pm 3°$, respectively (using propagation of errors). The errors on the

fractional intensities of Figs. 11–13 are on the order of ±12%.

3. Results

3.1. Circular dichroism measurements

The CD spectrum of holo-HSOD has been previously reported and its general features agrees with the fact that native HSOD is predominantly a β-sheet structure [1]. It was also shown that the CD spectra progressively decreases in magnitude as GdHCl concentration increases. Figure 1 shows the decrease of the relative amide and aromatic CD signal of holo-HSOD, θ_{220} and θ_{257}, monitored at 220 nm and 257 nm, respectively. As shown in Fig. 1, beyond 1–2 *M* GdHCl both signals progressively decrease in magnitude as GdHCl concentration increases. As a result, holo-HSOD is progressively denaturing with increasing GdHCl concentration. However, beyond 3.0 *M* GdHCl the tertiary structure signal (θ_{257}) decreases more quickly than the secondary structure signal (θ_{220}). In fact, beyond 4.5 *M* GdHCl the tertiary structure signal fluctuates about a small negative value while the secondary structure signal still continues to decrease. This non-parallel change in the tertiary structure CD relative to the secondary structure CD suggests the presence of an intermediate in holo-HSOD beyond 3.0 *M* GdHCl.

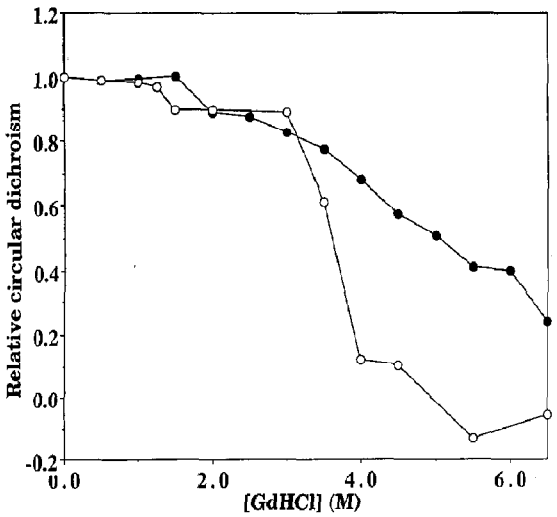

Fig. 1. Relative circular dichroism of holo-HSOD as a function of GdHCl concentration at 220 nm (●) and 257 nm (○). At 0.0 *M* GdHCl, $\theta_{220} = -1.053$ mdeg·cm^2·dmole^{-1} and $\theta_{257} = 0.0183$ mdeg·cm^2·dmole^{-1}. Relative CD was used to compare the GdHCl dependence of the two signals.

3.2. Time-resolved fluorescence decay measurements

Previous studies on native HSOD have shown that its time-resolved fluorescence decay is best described by a distribution of fluorescence lifetimes where the reasons for such a description have been previously discussed [1, 29, 30]. Of importance is the fact that the behavior of the lifetime distribution of HSOD as a function of temperature or denaturant is consistent with the hypothesis of conformational substates [21]. In particular, when the temperature of aqueous HSOD is decreased the width of its fluorescence lifetime distribution increases [30]. This behavior results from the reduced Trp interconversion rate between conformational substates as temperature is decreased. Consequently, at lower temperatures the Trp residue experiences each substate for a longer time than at higher temperatures. With respect to denaturant studies, it has been shown that the width of the fluorescence lifetime distribution of denatured HSOD is greater than that of native HSOD [1]. This is consistent with the expectation that more conformational substates are created upon denaturation of HSOD. On the basis of the above physical picture, we have analyzed, for this study, the time-resolved fluorescence decay of holo-HSOD using a Lorentzian lifetime distribution.

Figure 2 shows the resulting dependence of the lifetime distribution center as a function of GdHCl concentration and temperature using a single distributional component. Generally, the center of the lifetime distribution increases with decreasing temperature and increasing GdHCl concentration. The initial decrease of the center from 0.0 *M* to 1.0–2.0 *M* is due to a slight quenching effect of GdHCl on Trp. This effect has been confirmed by steady-state fluorescence

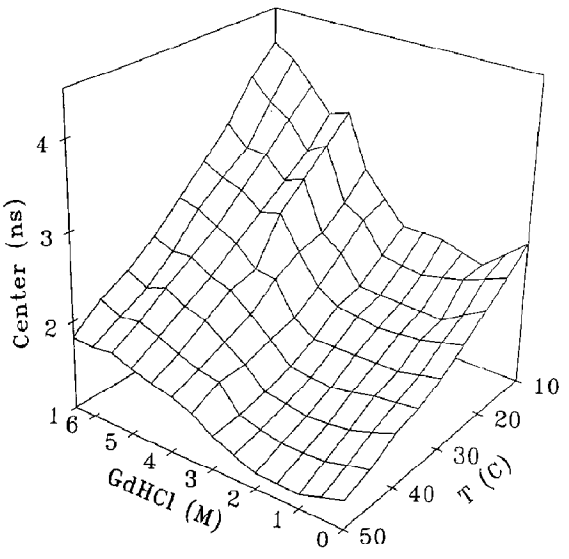

Fig. 2. Temperature and denaturant dependence of the center of the lifetime distribution of holo-HSOD.

intensity measurements on HSOD as a function of GdHCl concentration which shows an initial decrease from 0.0 *M* to 1.0–2.0 *M* GdHCl [1]. Preliminary experiments show that the unfolding of HSOD is partially reversible.

Figure 3 shows the temperature and denaturant dependence of the width of the fluorescence

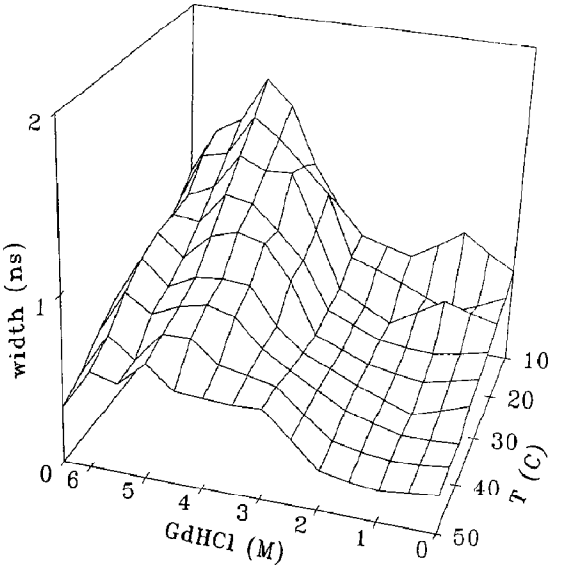

Fig. 3. Temperature and denaturant dependence of the width of the lifetime distribution of holo-HSOD.

lifetime distribution of HSOD for the analysis of Fig. 2. For all temperatures the denaturant dependence of the width agrees with our previous results at 20°C: (1) the width of denatured HSOD at 6.5 *M* GdHCl is greater than that of native HSOD, and (2) the width displays a maximum around 4.5–5.5 *M* GdHCl [1]. We have interpreted that the maximum of the distribution width observed between 4.5 and 5.5 *M* GdHCl as due to the presence of a monomer–dimer equilibrium in partially denatured HSOD [1]. A more detailed analysis of this equilibrium will be considered in the discussion. It should be noted, though, that HSOD in 0.0 or 6.5 *M* GdHCl does not display a monomer–dimer equilibrium (as monitored by its steady-state fluorescence anisotropy [1]). Thus, at 0.0 *M* GdHCl HSOD is a native dimer while at 6.5 *M* GdHCl HSOD is a denatured monomer.

3.3. Time-resolved fluorescence anisotropy measurements

The time-resolved anisotropy decay of HSOD, $r(t)$, for all temperatures and denaturant concentrations can be adequately described by two rotational correlation times,

$$r(t) = r_0\Big[A_\infty \exp\big(-t\phi_{\mathrm{pro}}^{-1}\big) + (1-A_\infty) \times \exp\big(-t\big(\phi_{\mathrm{pro}}^{-1} + \phi_{\mathrm{Trp}}^{-1}\big)\big)\Big], \quad (1)$$

where r_0 is the initial anisotropy, ϕ_{pro} is the rotational correlation time of the protein, ϕ_{Trp} is the rotational correlation time of the Trp residue and A_∞ is the square root of the order parameter of the Trp residue [31]. The r_0 value used for our analysis is the literature value of 0.278 for Trp excited at 295 nm [32]. Our results agree with previous results for the time-resolved anisotropy of aqueous HSOD as a function of GdHCl concentration at 20°C [1]. The use of two rotational correlation times (of which one is relatively short) can be interpreted as a Trp residue confined to free diffusion within a cone semi-angle θ while the whole protein molecule undergoes isotropic rotational diffusion [31]. This free diffusional ap-

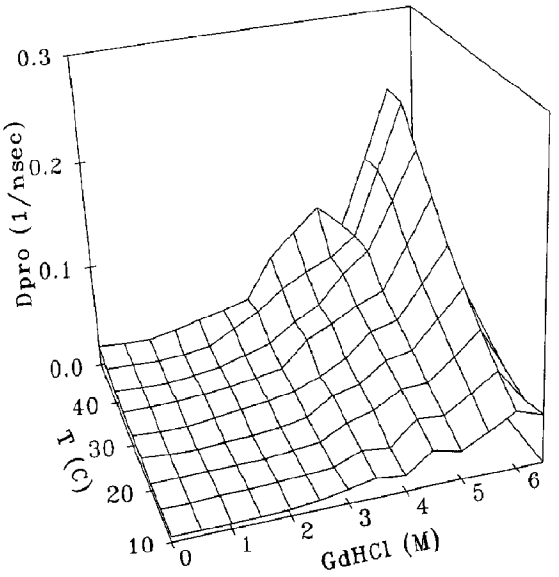

Fig. 4. Temperature and denaturant dependence of the rotational diffusion coefficient, D_{pro}, of holo-HSOD.

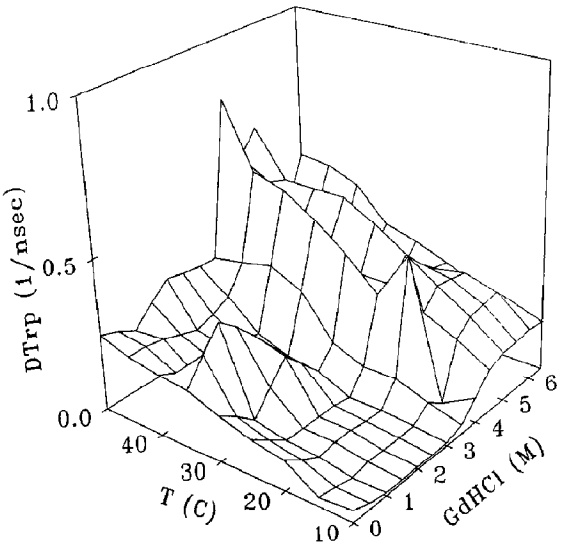

Fig. 5. Temperature and denaturant dependence of the tryptophan wobbling diffusion coefficient, D_{Trp}, of holo-HSOD.

proach is approximate considering that the Trp residue interconverts between conformational substates over a complex energy landscape.

Figure 4 shows the rotational diffusion coefficient, D_{pro}, of HSOD as a function of GdHCl concentration and temperature T. D_{pro} is calculated using the equation

$$D_{pro} = 1/(6\phi_{pro}), \tag{2}$$

At 0.0 M GdHCl, the volume of HSOD, V, can be estimated using the the Einstein–Stokes relation [33]

$$V = RT/6\eta D_{pro}, \tag{3}$$

where R is the gas constant, T is the temperature and η is the solvent viscosity. The obtained values of V range from 6.0×10^4 cm^3/mol at 10°C to 4.3×10^4 cm^3/mol at 50°C. Such values are compatible with the dry volume of HSOD (42,403 cm^3/mol [34]). As GdHCl concentration increases the values obtained for V becomes significantly lower than the dry volume of HSOD. Thus, the increase of D_{pro} with increasing GdHCl concentration is probably reflective of segmental motion.

Figures 5 and 6 show the temperature and denaturant dependence of the Trp wobbling diffusion coefficient, D_{Trp}, and the cone semi-angle θ, respectively. θ is obtained from

$$\theta = \arccos\left(\left(\sqrt{1 + 8\sqrt{A_\infty}} - 1\right)/2\right). \tag{4}$$

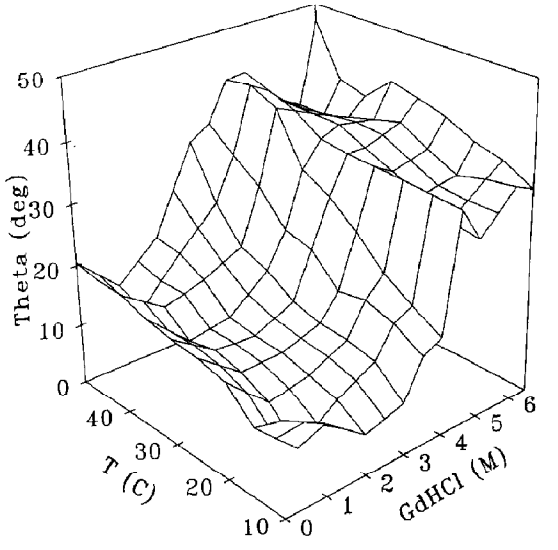

Fig. 6. Temperature and denaturant dependence of the cone semi-angle, θ, of holo-HSOD.

D_{Trp} is obtained from

$$D_{Trp}\theta_{Trp}(1-A_\infty) = -x^2(1+x)^2\{\log((1+x)/2) + ((1-x)/2)\}/2(1-x) + (1-x) \times(6+8x-x^2-12x^3-7x^4)/24, \quad (5)$$

where $x = \cos(\theta)$ [30,35]. The general trend from both figures is that from 3.0 *M* to 4.5 *M* GdHCl both parameters increase significantly. Beyond 4.5 *M* GdHCl, both parameters do not increase as much as below 4.5 *M* GdHCl.

4. Discussion

4.1. Evidence for structural microheterogeneity

The indication for structural microheterogeneity came about from our previous study of HSOD [1]. Structural heterogeneity here indicates a relatively stable conformational difference between protein molecules in the ensemble. The microheterogeneity can be observed for periods longer than the experimental time (which is in hours). A summary of the observations leading to this conclusion is now in order: (1) at 3.5 GdHCl the steady-state anisotropy, $\langle r \rangle$, of HSOD varies with protein concentration, (2) in contrast to the steady-state anistropy, the amide CD signal is constant over a wide range of HSOD concentration at all GdHCl concentrations, (3) the center of the lifetime distribution is relatively constant over the same range of HSOD concentration in 3.5 *M* GdHCl and (4) the width of the lifetime distribution increases as HSOD concentration decreases in 3.5 *M* GdHCl. One final note is that the time-resolved fluorescence decay of HSOD, when all denaturant concentrations are considered, cannot be due to a sum contribution from native and denatured species only [1]. These observations lead to the model which is schematically shown in Fig. 7 . Figure 7 shows the experimental directions one can take the HSOD system: (1) along the denaturant axis, and (2) along the protein concentration axis (referred to as the dilution axis). The native HSOD system consists

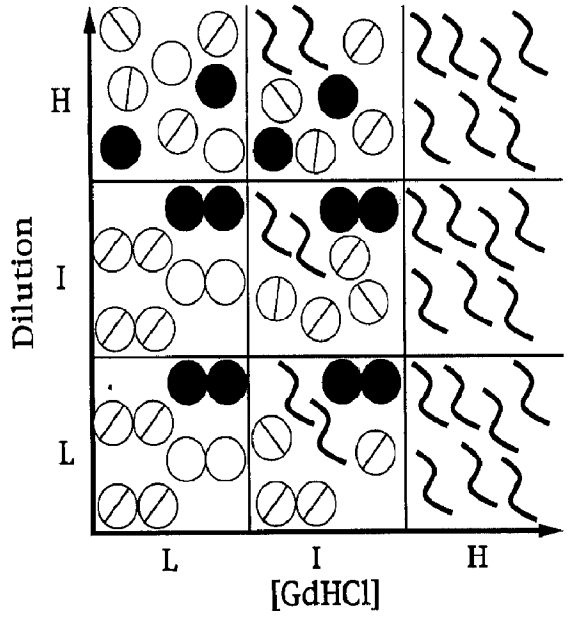

Fig. 7. Schematic portrayal of the holo-HSOD population subject to various degrees of GdHCl concentration, [GdHCl], and dilution. L, I and H denotes low, intermediate and high, respectively. The paired filled circles are strong proteins referred to as species S. The paired circles cut by a line are weak proteins referred to as species W. The paired empty circles are protein molecules easily denatured at intermediate [GdHCl]. The denatured monomer is portrayed as a random coil and referred to as species U. The single circles cut by a line are monomers originating from species W and referred to as species M. The single filled circles are monomers originating from species S.

of dimers at the origin of Fig. 7. However, if the system is subject to an intermediate denaturant concentration then, due to population microheterogeneity, some proteins are more stable and resist complete denaturation while other molecules denature. However, at this denaturant concentration, there are protein molecules that are stable enough to remain native yet at the same time they are susceptible to monomerization. This equilibrium can be explored by moving along the dilution axis of Fig. 7. The situation portrayed in Fig. 7 explains why the amide CD signal does not change upon dilution, since the population of unfolded proteins remains the same at all values along the dilution axis. Dilution also gives rise to a decrease in $\langle r \rangle$. However, the width of the lifetime distribution increases with increasing dilution and this suggests that the

monomers do not have the same structural integrity as the dimers.

Each of the species in Fig. 7 has a characteristic fluorescence lifetime distribution and it is possible to decompose the time- resolved fluorescence of HSOD as a sum of three species while satisfying previous fluorescence observations as a function of HSOD concentration. We assumed that the fluorescence lifetime distribution of species S and U can be obtained from lifetime measurements at 0.0 *M* and 6.5 *M* GdHCl, respectively. It has been shown that at very high protein concentration the width of the lifetime distribution of holo-HSOD in 3.5 *M* GdHCl is close to that of native holo-HSOD. This suggests that the width of species W is similar to that of species S. Since species W is a dimer it is reasonable to assume that the center of the lifetime distribution of W is the same as S. The task now remains to obtain the lifetime parameters of species M as well as the fractional intensity contribution of each species to the time- resolved fluorescence decay of HSOD at a given denaturant concentration.

For this goal, the time-resolved fluorescence decay of HSOD at a given GdHCl concentration is described as a sum of three Lorentzian distributions: (1) strong dimers plus weak dimers with a lifetime distribution center, c_N, and a lifetime distribution width w_N, (2) monomers with a lifetime distribution center, c_M, and a lifetime distribution width w_M, and (3) denatured monomers with a lifetime distribution center, c_U, and a lifetime distribution width w_U. We denote species N as the sum combination of species S and W. Thus, N represents native protein molecules. Species M denotes the monomer and species U denotes the unfolded monomers. A global fit over GdHCl concentration was performed for a particular temperature T with the parameters w_N, c_M, w_M, c_U and w_U linked. The only free parameters in the fit are c_M, w_M and the percentage of fractional intensity, f_N, f_M and f_U for species N, M, and U, respectively.

Due to a quenching effect of GdHCl on HSOD c_N decreases roughly 0.2–0.4 ns from 0.0 to 1.0–3.0 *M* GdHCl. Beyond this range of GdHCl concentration species N becomes relatively unpopulated and c_N can be set to essentially a constant which is roughly the least value attained during the quenching process. The resulting fit shows that c_M has a value close to c_N. Using this model we obtained a GdHCl dependence of the center of the lifetime distribution of species N, M and U at 15°C in Fig. 8. The starting and ending of these curves (from left to right along the GdHCl axis) signifies the appearance and disappearance, respectively, of a particular species. The unfolded species U has a large value for c_U probably due to the distancing of the Trp residue from quenching groups in the native configuration. The recovered value of w_M obtained at 15°C was 1.4 ns with an error of about ±0.2 ns. For all temperatures, the denaturant behavior of c_N, c_M and c_U are similar to that of Fig. 8. Figure 9 shows the resulting fractional intensity, f_N, f_M and f_U for HSOD at 15°C as a function of GdHCl concentration. As shown in Fig. 9, species N decreases with increasing denaturant concentration, species U increases with increasing denaturant concentration and species M increases from 2.0 to 5.0 *M* GdHCl and then decreases to 0 beyond 5.0 *M* GdHCl. Figure 10 shows the thermal behavior of the width of the three species. Generally, w_M is greater than w_N and w_U. Though w_M has a more complex temperature behavior than w_N and w_U,

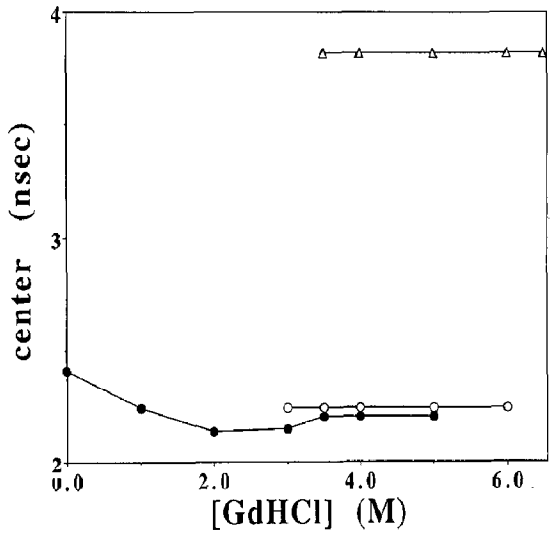

Fig. 8. Denaturant dependence of the center of the lifetime distribution of native (●), monomer (empty circles) and unfolded (△) species of HSOD at 15°C.

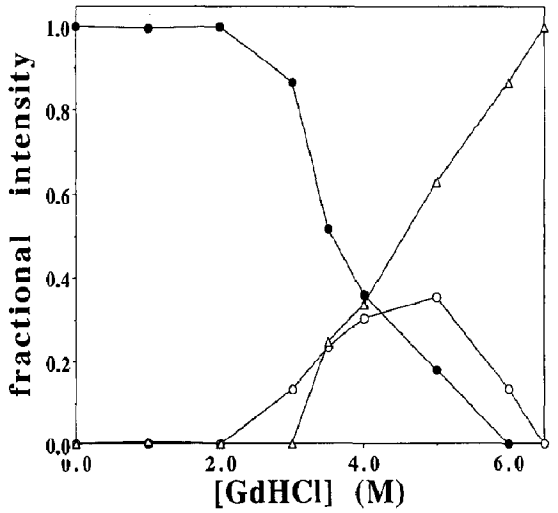

Fig. 9. Denaturant dependence of fractional intensity of native (●), monomer (○) and unfolded (△) species of HSOD at 15°C.

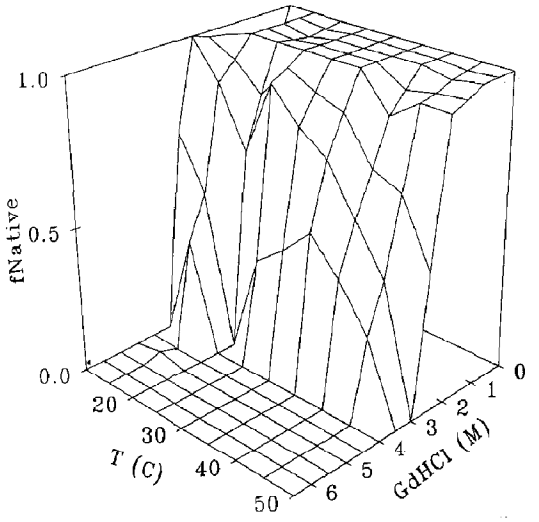

Fig. 11. Denaturant and temperature dependence of the percentage fractional intensity of the native species of HSOD.

it generally decreases with increasing temperature. Figure 11, 12 and 13 shows the three-dimensional graphs of f_N, f_M and f_U, respectively, as a function of GdHCl concentration and temperature. At all temperatures, the denaturant behavior of f_N, f_M and f_U are similar to that of Fig. 9.

The decomposition shows that w_M is greater than w_N which agrees with the fact that the width of the lifetime distribution of HSOD in 3.5 *M* GdHCl increases with dilution. Furthermore, $c_M \approx c_N$ which agrees with the relatively constant behavior of the center of the lifetime distribution of HSOD in 3.5 *M* GdHCl for all protein concentrations. Figure 12 shows that the occurrence of a maximum in the width of the lifetime distribution

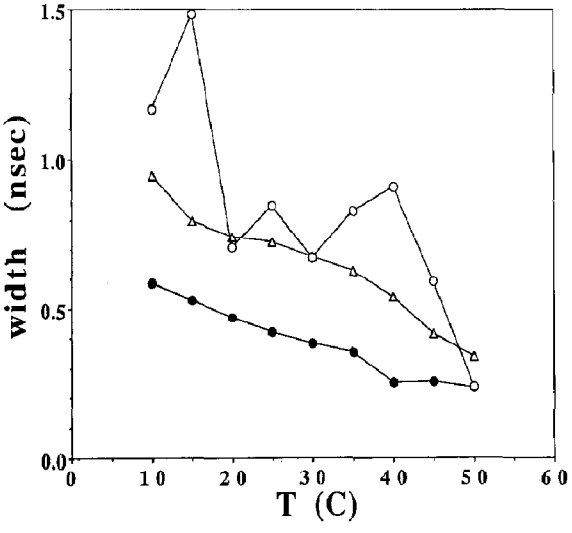

Fig. 10. Temperature dependence of the width of the lifetime distribution of native (●), monomer (○) and unfolded (△) species for HSOD.

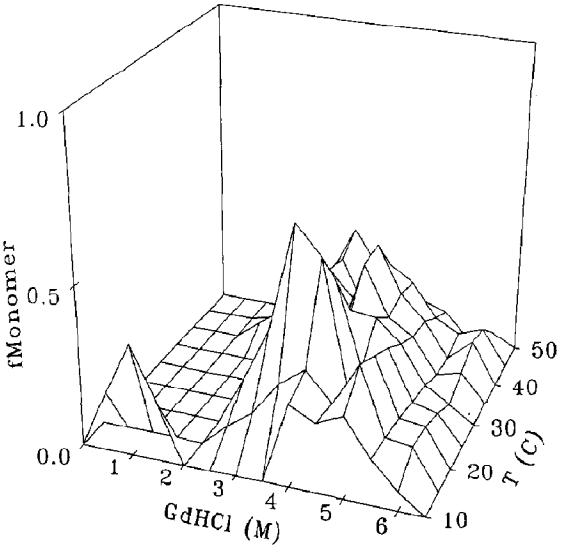

Fig. 12. Denaturant and temperature dependence of the percentage fractional intensity of the monomer species of HSOD.

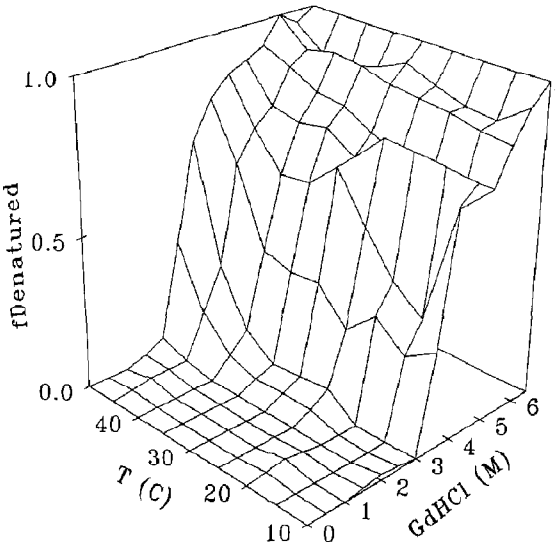

Fig. 13. Denaturant and temperature dependence of the percentage fractional intensity of the unfolded species of HSOD.

in Fig. 3 is due to the occurrence of a maximum in the concentration of species M. The above decomposition provides independent verification of an intermediate state in the unfolding of HSOD which is in agreement with the fluorescence characteristics features of species M inferred from the protein concentration dependent experiments [1]. It is interesting to note that the sharp drop in the aromatic CD of HSOD (around 3.0–3.5 *M* GdHCl) roughly coincides with the sharp changes in (1) the width of Fig. 3, (2) segmental motion portrayed in Fig. 5 by D_{pro}, and (3) D_{Trp} and θ of Figs. 6 and 7, respectively. This suggests that the time-resolved parameters of holo-HSOD indicate increased structural microheterogeneity in the protein population about 3.0–3.5 *M* GdHCl. Furthermore, since the width of the lifetime distribution increases with dilution (at intermediate GdHCl concentrations) while the amide CD is constant this further suggests that the monomer designated as M displays this molten globule state, i.e. it retains its native secondary structure while displaying fluid- like tertiary structure. From our decomposition as well as our time-resolved anisotropy measurements we list the following native and fluid like characteristics of partially denatured HSOD which support species M as being a molten globule state.

4.1.1. Native-like environment about the Trp residue

The resulting global decomposition of the time-resolved fluorescence of HSOD as a function of GdHCl which showed that the center of the lifetime distribution of species M is similar to that of the native state (Fig. 8). As a result the average environment of the Trp residue for species M is similar to that of the native state.

4.1.2. Segmental motion increases from 0.0 to 6.0 M GdHCl

As shown in Fig. 4 the increase of D_{pro} with GdHCl concentration is indicative of segmental motion. Clearly D_{pro} has its contribution from U and probably the decrease of D_{pro} from 6.0 *M* to 6.5 *M* GdHCl is due to the elimination of M species. However, the fact that D_{pro} does continue to increase from 0.0 to 6.0 *M* GdHCl is suggestive that species M also has fluid-like segmental motion.

4.1.3. Large fluidity of the environment about Trp

As shown in Figs. 5 and 6 major increases in D_{Trp} and θ occur between 3.0 and 4.5 *M* GdHCl. After 4.5 *M* GdHCl both parameters do not change as much. Considering, from Figs. 11–13, that only species W and U probably exist beyond 4.0–5.0 *M* GdHCl, Figs. 5 and 6 suggest that the fluidity of the Trp environment of species W is similar to that of species U. In particular, the high value of θ after 4.5 *M* GdHCl provides the Trp residue with large freedom to diffuse. At the same time, the large value of D_{Trp} suggests that there are less barriers to impede the diffusion of Trp.

4.1.4. Increased heterogeneity of the system upon monomerization

The global decomposition of the time-resolved fluorescence of HSOD shows that the width of the lifetime distribution of species M is generally greater than that of the unfolded and native species (Fig. 10). The reason why the width for species M is greater than that of the native species is due to the greater number of conformational substates in M. This would be compatible with the suggestion that M displays fluctuating tertiary structure.

In terms of the potential surface of HSOD (as a function of conformational coordinate) more substates are created at intermediate GdHCl concentrations while a majority of the energy barriers separating these substates remains relatively high. This physical situation yields a very heterogeneous time-resolved fluorescence decay for HSOD about 4.5–5.5 *M* GdHCl. We believe this stage is characteristic of species M. However, increasing denaturant concentration promotes increased segmental motion that likely arises from decreasing the energy barriers between conformational substates. As a result, the Trp-protein system can interconvert quickly between substates yielding a less heterogeneous fluorescence decay at 6.5 *M* GdHCl.

5. Conclusions

In summary, it can be seen that structural microheterogeneity can explain the time-resolved fluorescence decay of holo-HSOD as a function of denaturant concentration and temperature. Furthermore, CD, fluorescence measurements and global analysis reveals an HSOD unfolding intermediate. In particular, it can be reasoned that species M has native-like characteristics in its secondary structure and average quenching environment while at the same time its molten characteristics take the form of increased fluidity and increased heterogeneity in its time-resolved fluorescence decay. Such observations strongly suggest that the monomerization stage of HSOD displays a molten globule state.

Acknowledgments

The Laboratory for Fluorescence Dynamics members are supported by the Division of Research Resources of the National Institute of Health (RR03155) and by the University of Illinois at Urbana- Champaign. This work was also supported by the Italian National Research Council (CNR), Target project "Biotechnology and Bioinstrumentation".

References

1 G. Mei, N. Rosato, N. Silva, R. Rusch. E. Gratton, I. Savini and A. Finazzi-Agrò, Biochemistry 31 (1992) 7224–7230.
2 D. Dressler and H. Potter, Discovering enzymes (W.H. Freeman, New York, 1991) pp. 205–207.
3 V.E. Bychkova, R.H. Pain and O.B. Ptitsyn, FEBS Lett. 238 (1988) 231–234.
4 T.E. Creighton, Prog. Biophys. Mol. Biol. 33 (1978) 231–297.
5 K. Kuwajima, Proteins Struct. Funct. Genet. 6 (1989) 87–103.
6 H. Christensen and R.H. Pain, Eur. Biophys. J. 19 (1991) 221–229.
7 J.S. Weissman and P.S. Kim, Science 253 (1991) 1386–1393.
8 P.S. Kim and R.L. Baldwin, Annu. Rev. Biochem. 51 (1982) 459–489.
9 R. Lumry, R. Biltonen, and J. Brandts, F. Biopolymers 4 (1966) 917–944.
10 O.B. Ptitsyn, and T.M. Birshtein, Biopolymers 7 (1969) 435–445.
11 O.B. Ptitsyn, J. Prot. Chem. 6 (1987) 273–293.
12 J.M. Beechem, Proc. SPIE 1640 (1992) 676–680.
13 A. Grinvald and I.Z. Steinberg, Biochim. Biophys. Acta 427 (1976) 663–678.
14 Y. Saito, H. Tachibana, H. Hayashi and A. Wada, Photochem. Photobiol. 33 (1981) 289–295.
15 I. Gryczynski, M. Eftink and J.R. Lakowicz, Biochim. Biophys. Acta 954 (1988) 244–252.
16 E. Bismuto, E. Gratton and G. Irace, Biochemistry 27 (1988) 2132–2136.
17 D. Amir, S. Krausz and E. Haas, Proteins Struct. Funct. Genet. 13 (1992) 162–173.
18 E.D. Getzoff, J.A. Tainer, M.M. Stempien, G.I. Bell and R.A. Hallewell, Proteins Struct. Funct. Genet. 5 (1989) 322–336.
19 H. Frauenfelder, F. Parak and R.D. Young, Annu. Rev. Biophys. Biophys. Chem. 17 (1988) 451–479.
20 H. Frauenfelder, S.G. Sligar and P.G. Wolynes, Science 254 (1991) 1598–1603.
21 J.R. Alcala, E. Gratton and F.G. Prendergast, Biophys. J. 51 (1987) 925–936.
22 D.A. Dolgikh, R.I. Gilmanshin, E.V. Brazhnikov, V.E. Bychkova, G.V. Semisotnov, S.Y. Venyaminov and O.B. Ptitsyn, FEBS Lett. 136 (1981) 311–315.
23 J.D. Bryngelson and P.G. Wolynes, Proc. Natl. Acad. Sci. USA 84 1989) 7524–7528.
24 J.V. Bannister and W.H. Bannister, Meth. Enzymol. 105 (1984) 88–93.
25 E. Gratton and D.M. Jameson, R. Hall, Annu. Rev. Biophys. Bioeng. 13 (1984) 105–124.
26 E. Gratton and M. Limkeman, Biophys. J. 44 (1983) 315–324.
27 D.V. O'Conner and D. Phillips, Time-correlated single photon counting, 1st edn. (Academic Press, New York, 1984) pp. 257–261.

28 J.M. Beechem and E. Gratton, Proc. SPIE 909 (1988) 70–81.
29 N. Rosato, G. Mei, E. Gratton, J.V. Bannister, W.H. Bannister and A. Finazzi-Agrò, Biophys. Chem. 36 (1990) 41–46.
30 N. Rosato, E. Gratton, G. Mei and A. Finazzi-Agrò, Biophys. J. 58 (1990) 817–822.
31 G. Lipari and A. Szabo, Biophys. J. 30 (1980) 489–506.
32 B. Valeur and G. Weber, excitation bands. Photochem. Photobiol. 25 (1977) 441–444.
33 A. Einstein, Ann. Physik 19 (1906) 371–381.
34 H.E. Parge, E.D. Getzoff, C.S. Scandella, R.A. Hallewell and J.A. Tainer, J. Biol. Chem. 261 (1986) 16215–16218.
35 K. Kinosita, S. Kawato and A. Ikegami, Biophys. J. 20 (1977) 289–305.